https://doi.org/10.5194/egusphere-2023-322
Preprint. Discussion started: 24 March 2023

Enrichment of calcium in sea spray aerosol through bulk measurements and individual particle analysis during the R/V *Xuelong* cruise over the Ross Sea, Antarctica

Bojiang Su [a, b], Xinhui Bi [a, c], Zhou Zhang [b, d], Yue Liang [e], Congbo Song [f], Tao Wang [a, b], Yaohao Hu [a, b], Lei Li [g, *], Zhen Zhou [g], Jinpei Yan [h], Xinming Wang [a, c], Guohua Zhang [a, c, *]

[a] State Key Laboratory of Organic Geochemistry and Guangdong Provincial Key Laboratory of Environmental Protection and Resources Utilization, Guangzhou Institute of Geochemistry, Chinese Academy of Sciences, Guangzhou 510640, China

[b] University of Chinese Academy of Sciences, Beijing 100049, China

[c] Guangdong-Hong Kong-Macao Joint Laboratory for Environmental Pollution and Control, Guangzhou 510640, China

[d] State Key Laboratory of Isotope Geochemistry, Guangzhou Institute of Geochemistry, Chinese Academy of Sciences, Guangzhou 510640, China

[e] Department of Civil and Environmental Engineering, Faculty of Science and Technology, University of Macau, Taipa, Macau, China

[f] National Centre for Atmospheric Science (NCAS), University of Manchester, Manchester M13 9PL, UK

[g] Institute of Mass Spectrometry and Atmospheric Environment, Jinan University, Guangzhou 510632, China

[h] Key Laboratory of Global Change and Marine–Atmospheric Chemistry, Third Institute of Oceanography, Ministry of Natural Resources, Xiamen 361005, China

*Corresponding author: zhanggh@gig.ac.cn; lileishdx@163.com

https://doi.org/10.5194/egusphere-2023-322
Preprint. Discussion started: 24 March 2023

Abstract: Calcium is known to be enriched in sea spray aerosols (SSA), but its controlling factors and individual mixing states remain ambiguous. Here, we investigate the impact of various environmental factors on the water-soluble calcium (Ca^{2+}) distribution in SSA through R/V *Xuelong* cruise observations over the Ross Sea, Antarctica, from December 2017 to February 2018. We observed enhanced Ca^{2+} enrichment in aerosol samples at lower temperatures (< -3.5 ℃), lower wind speeds (< 7 m s^{-1}) and in the presence of sea ice. Further individual particle mass spectral analysis indicated that considerable fractions of calcium in SSA likely bind with organic matter (a single-particle type, OC-Ca), which may be neglected in current water-soluble estimation of Ca^{2+} enrichment. Also, this is the first time that a calcium-dominated single-particle type has been observed in the Antarctic atmosphere. We suggest that a broader focus on individual OC-Ca and its subsequent environmental behavior should be included in future Antarctic atmospheric modeling. Given the context of global warming and sea ice retreat, an understanding of the mechanisms of calcium enrichment and mixing state of individual particles involved is valuable for further recognizing the aerosol-cloud-climate interactions in the Antarctica summer.

https://doi.org/10.5194/egusphere-2023-322
Preprint. Discussion started: 24 March 2023

Key points:

- Enhanced Ca^{2+} enrichment in sea spray aerosol (SSA) was observed at lower ambient temperatures, lower wind speeds and in the presence of sea ice.
- Individual particle analysis revealed a large proportion of internally mixed organics with calcium particles in the Antarctic summer atmosphere.
- Organically complexed calcium may be neglected in current water-soluble estimation of Ca^{2+} enrichment in SSA.

Key worlds: Sea spray aerosol; Calcium enrichment; Individual particle analysis; Environmental factors; Internally mixed organics with calcium particles; Antarctic summer atmosphere.

https://doi.org/10.5194/egusphere-2023-322
Preprint. Discussion started: 24 March 2023

1 Introduction

Sea spray aerosol (SSA) govern radiative forcing by directly scattering and absorbing solar radiation over the remote ocean (Murphy et al., 1998), and they affect the microphysical properties of marine clouds by serving as cloud condensation nuclei (CCN) and ice nuclei (IN) (Wilson et al., 2015; Brooks and Thornton, 2018; Willis et al., 2018). Calcium is one of the components of SSA, which can present as inorganic calcium (e.g., $CaCl_2$ and $CaSO_4$) (Chi et al., 2015) as well as organic calcium (i.e., the most efficient gelling agent) (Quinn et al., 2015; Bertram et al., 2018; Carter-Fenk et al., 2021). The extent of enrichment and chemical signature of calcium may affect some physicochemical properties of SSA such as alkalinity and hygroscopicity (Salter et al., 2016; Mukherjee et al., 2020), which is critical for understanding aerosol-cloud interactions over the remote marine boundary layer (Keene et al., 2007; Leck and Svensson, 2015; Bertram et al., 2018).

A growing number of studies have shown that calcium (Ca^{2+}) is significantly enriched in SSA relative to bulk seawater (Table S1) (Keene et al., 2007; Hara et al., 2012; Cochran et al., 2016; Salter et al., 2016; Cravigan et al., 2020; Mukherjee et al., 2020). For example, Hara et al. (2012) found that the Ca^{2+} enrichment of aerosol samples was sensitive to sea salt fractionation during the cold winter-spring season over the Antarctic coast. Leck and Svensson (2015) suggested that Ca^{2+} enrichment in SSA is attributed to bubble bursts on sea ice leads within the sea ice over the Arctic area. Similarly, low wind-driven bubble bursts were regarded as a major reason for the Ca^{2+} enrichment in SSA during an Arctic cruise (Mukherjee et al., 2020). These results have greatly improved the understanding of the processes contributing to Ca^{2+} enrichment; however, our

https://doi.org/10.5194/egusphere-2023-322
Preprint. Discussion started: 24 March 2023

understanding of how environmental factors synergistically affect such enrichment processes remains unclear.

The enrichment extent of calcium and its chemical form in SSA have been deduced with water-soluble Ca^{2+}. Two hypotheses have been proposed: (i) calcium enrichment is dominated by inorganic calcium, such as $CaCl_2$ and $CaCO_3 \cdot 6H_2O$ (ikaite), derived from wind-blown bubble bursts, calcareous shell debris and/or sea salt fractionation (Keene et al., 2007; Dieckmann et al., 2008; Hara et al., 2012). (ii) Ca^{2+} may bind with organic matter, which is relevant with marine microgels and/or coccolithophore phytoplankton scales, and can be emitted by bubble bursting (Oppo et al., 1999; Sievering, 2004; Leck and Svensson, 2015; Cochran et al., 2016; Kirpes et al., 2019; Mukherjee et al., 2020). The chemical form of calcium can significantly determine its atmospheric role, and inorganic calcium may exhibit stronger aerosol alkalinity and hygroscopicity than organic calcium (Salter et al., 2016; Mukherjee et al., 2020). However, because organic calcium has low water solubility (e.g., aged Ca^{2+}-assembled gel-like particles) (Orellana and Verdugo, 2003; Leck and Bigg, 2010; Russell et al., 2010; Orellana et al., 2011; Leck and Svensson, 2015), the commonly measured water-soluble Ca^{2+} may not precisely explain the calcium distribution in SSA. Thus, an understanding of the mixing state of individual calcareous aerosols may provide unique insight into the mechanisms of calcium enrichment in SSA.

As a part of the 34th Chinese Antarctic Research Expedition (CHINARE ANT34th), the aim of this study was to investigate the influencing factors and possible mechanisms of calcium enrichment in SSA through R/V *Xuelong* cruise observations over the Ross Sea, Antarctica. An in situ gas and aerosol composition monitoring system (IGAC) was employed to determine the

https://doi.org/10.5194/egusphere-2023-322
Preprint. Discussion started: 24 March 2023

extent of Ca^{2+} enrichment in SSA. Single-particle aerosol mass spectrometry (SPAMS) was utilized to measure the size and chemical signature (i.e., mixing state) of individual calcareous particles. We first investigated the impact of environmental factors such as ambient temperature, wind speed, sea ice fraction, and chlorophyll-a concentration on Ca^{2+} enrichment in SSA. Then, the mechanisms of calcium enrichment in SSA were inferred according to the mixing state of individual calcareous particles.

2 Methodology

2.1 The R/V *Xuelong* cruise and observation regions

Two observations were carried out aboard the R/V *Xuelong* cruise over the Ross Sea, Antarctica (50 to 78° S, 160 to 185° E) (Fig. S1). During sampling, this region was relatively isolated from the impact of long-range transport of anthropogenic aerosols and has experienced the sea ice retreat (Yan et al., 2020a). The first leg of the cruise (leg I) was conducted from 2-20 December, 2017, when the ocean was covered by sea ice. The second leg of the cruise (leg II) was carried out in the same region from January 13 to February 14, 2018, when basically no sea ice presents. Therefore, legs I and II were also regarded as the "sea ice period" and "the period without sea ice", respectively, hereafter.

2.2 Metrological parameters and satellite data of air masses, sea ice and chlorophyll-a

Meteorological parameters, including ambient temperature, relative humidity (RH), wind speed, and true wind direction were measured by an automated meteorological station on the top deck of the R/V *Xuelong* (Fig. S2 and Table S2).

https://doi.org/10.5194/egusphere-2023-322
Preprint. Discussion started: 24 March 2023

The type of air masses was calculated by 72-hour back trajectory analysis using the NOAA Hybrid Single-Particle Lagrangian Integrated Trajectories (HYSPLIT, version 4.9) model (Fig. S1). The monthly sea ice fraction was obtained from the Sea Ice Concentration Climate Data Record with a spatial resolution of 25 km (https://www.ncei.noaa.gov/products/climate-data-records/sea-ice-concentration). The 8-day chlorophyll-a concentration was collected from MODIS-aqua with a spatial resolution of 4 km (https://modis.gsfc.nasa.gov) (Fig. S3).

During the R/V *Xuelong* cruise observations, leg I was dominantly affected by the 72-h air masses from the sea ice-covered open-water (78%), and leg II was mainly affected by the 72-h air masses from continental Antarctica (40%) (Fig. S1 and Table S1). The average ambient temperature (-4.0 ± 1.4 ℃ vs. -3.1 ± 2.2 ℃), wind speed (7.2 ± 5.5 m s^{-1} vs. 7.1 ± 4.2 m s^{-1}), and chlorophyll-a concentration (0.51 ± 0.29 μg L^{-1} vs. 0.44 ± 0.18 μg L^{-1}) varied slightly between legs I and II (Table S2).

2.3 Instrumentation

2.3.1 Aerosol water-soluble ion constituents

An IGAC (Model S-611, Machine Shop, Fortelice International Co. Ltd., Taiwan, China) was applied to determine the water-soluble ion mass concentrations of aerosol (Fig. S4). Notably, only the water-soluble fraction (organic and inorganic) of the aerosols sampled was considered (details in Supporting Information, SI text S1) (Oppo et al., 1999). Sampling was performed only while the ship was sailing. A PM_{10} cyclone was fixed to a bow mast at 20 m above the sea surface for IGAC sampling to minimize the impact of stern emissions. The details of the analytical method and ion mass concentrations have been described in previous studies (SI Text S2 and (Yan et al.,

https://doi.org/10.5194/egusphere-2023-322
Preprint. Discussion started: 24 March 2023

2019; Yan et al., 2020b)). Briefly, the gases and aerosols are separated and converted into liquid effluent by a Wet Annular Denuder and a Scrub and Impact Aerosol Collector. Each sample was collected for 55 minutes and injected for 5 minutes. Subsequently, an ion chromatography (IC) system (Dionex ICS-3000) within IGAC was used to analyze the water-soluble species of aerosol samples in one-hour resolution, with the systematic error below 5%. The target ion concentrations were calibrated with a coefficient of determination (r^2) above 0.99 by using standard solutions. The detection limits for Na^+, Cl^-, Ca^{2+}, K^+, and Mg^{2+} were 0.03, 0.03, 0.019, 0.011, and 0.042 μg L^{-1} (aqueous solution), respectively. During the whole observations, the mean Na^+ and Ca^{2+} mass concentrations were 364.64 ng m^{-3} (ranging from 6.66 to 4580.10 ng m^{-3}) and 21.20 ng m^{-3} (ranging from 0.27 to 334.40 ng m^{-3}), respectively, which were far above (> 10 times) the detection limits. In comparison with the whole measurement (21.2 ng m^{-3}), the mean Ca^{2+} mass concentrations were lower at low wind speeds (17.3 ng m^{-3} at < 7 m s^{-1} and 15.0 ng m^{-3} at < 3m s^{-1}). Therefore, the impact of ship emissions on the Ca^{2+} mass concentration could be negligible under the low wind conditions. Analytical uncertainty of Ca^{2+} enrichment based on water-soluble analysis estimated less than 11% (SI text S3).

2.3.2 Single-particle analysis

The size and chemical signature of individual particles were obtained in real-time by a SPAMS (Hexin Analytical Instrument Co., Ltd., China) (Fig. S4). A brief description of the SPAMS is provided elsewhere (SI Text S2 and (Li et al., 2011)). Briefly, the aerosols were drawn into SPAMS by a $PM_{2.5}$ inlet after a silica gel dryer. A collimated particle beam focused by an aerodynamic lens is then accelerated in an accelerating electric field and passed through two

https://doi.org/10.5194/egusphere-2023-322
Preprint. Discussion started: 24 March 2023

continuous laser beams (Nd: YAG laser, 532 nm). The obtained time of flight (TOF) and velocity of individual particles were used to calculate the vacuum aerodynamic diameter (D_{va}) based on a calibration curve. Subsequently, particles with a specific velocity were desorbed and ionized by triggering a pulse laser (an Nd: YAG laser, 266 nm, 0.6 ± 0.06 mJ was used in this study). The ion fragments were recorded using a TOF mass spectrometer. Prior to the use of SPAMS, standard polystyrene latex spheres (0.2-2 μm, Duke Scientific Corp., Palo Alto, CA) and $PbCl_2$ and $NaNO_3$ (0.35 μm, Sigma-Aldrich) solutions were used for the size and mass spectral calibration, respectively. The hit rate, defined as the ratio of ionized particles to all sampled particles, of the SPAMS is ~ 11% during the cruise observation.

During the R/V *Xuelong* cruise observations, approximately 930,000 particles with mass spectral fingerprints and D_{va} ranging from 0.2 to 2 μm were measured. An adaptive resonance theory neural network (ART-2a) grouped the particles into several clusters based on their mass spectral fingerprints, using parameters of a vigilance factor of 0.85, a learning rate of 0.05, and a maximum of 20 iterations (Song and Hopke, 1999). The manually obtained clusters were sea salt (SS, 16.5%), aged sea salt (SS-aged, 8.1%), sea salt with biogenic organic matter (SS-Bio, 3.1%), internally mixed organics with calcium (OC-Ca, 48.7%), internally mixed organics with potassium (OC-K, 13.7%), organic-carbon-dominated (OC, 7.0%), and element carbon (EC, 2.9%) (Fig. S5 and Table S3) (Prather et al., 2013; Collins et al., 2014; Su et al., 2021). All single-particle types had marine origins with typical mass spectral characteristics of Na (*m/z* 23), Mg (*m/z* 24), K (*m/z* 39), Ca (*m/z* 40), and Cl (*m/z* -35 and -37), except for EC (SI text S4).

https://doi.org/10.5194/egusphere-2023-322
Preprint. Discussion started: 24 March 2023

3 Results

3.1 Ca^{2+} enrichment dominated by environmental factors

The enrichment factor (EFx), defined as the mass concentration ratio of a specific species X to Na^+ in aerosols to that in bulk seawater, is generally used to describe the enrichment extent of species X in aerosols.

$$EFx = \frac{([X]/[Na^+])_{aerosol}}{([X]/[Na^+])_{seawater}}$$

An EFx > 1 indicates a positive enrichment; otherwise, it indicates depletion. The measurements were almost entirely influenced by polar air masses (Fig. S1). Therefore, the long-range transport of anthropogenic aerosols may be limited. All Na^+ was assumed to originate from SSA. Generally, the ratio of Ca^{2+} to Na^+ in seawater is 0.038 (w/w) (Boreddy and Kawamura, 2015; Su et al., 2022). During the whole cruise, the hourly average EF_{Ca} was 2.76 ± 6.27 (mean ± standard deviation (M ± SD), n = 1051, ranged from 0.01 to 85, median =1.18, interquartile range (IQR) = 1.85). Similar to previous studies (Salter et al., 2016), positive magnesium (Mg^{2+}) and potassium (K^+) enrichment in SSA was also observed (SI text S5).

Figure 1 shows the enrichment factor of Ca^{2+} (EF_{Ca}) at different ambient temperatures (separated by a mean value of -3.5 ℃), wind speeds (separated by a mean value of 7 m s^{-1}), and with/without sea ice during the whole cruise. The results clearly indicated that the highest EF_{Ca} zone (M ± SD = 3.83 ± 3.43, median = 2.66, IQR = 3.37, n = 144) appeared at a relatively low ambient temperature (< -3.5 ℃), low wind speed (< 7 m s^{-1}) and in the presence of sea ice (Fig. S6). The EF_{Ca} increased with decreasing ambient temperature and wind speed, as also shown in Fig. 2. In addition, the positive Ca^{2+} enrichment events (71%) were most associated with leg I, that

https://doi.org/10.5194/egusphere-2023-322
Preprint. Discussion started: 24 March 2023

is, air masses blowing from the large fraction of sea-ice-covered ocean (i.e., Ross Sea, 78%) (Table S1). And there was a positive correlation ($r = 0.73$, $p < 0.01$) between the sea ice fraction and EF_{Ca} during leg I (sea ice period) (Fig. 2), indicating a possible effect of the presence of sea ice on Ca^{2+} enrichment in SSA. Under the conditions of ambient temperatures < -3.5 ℃ and wind speeds < 7 m s^{-1}, a higher EF_{Ca} was observed during the sea ice period than during the period without sea ice (3.83 ± 3.43 vs. 2.45 ± 3.09 by M ± SD and 2.66 vs. 1.18, by median) (Fig. S6). In contrast, under the conditions of ambient temperatures ≥ -3.5 ℃, wind speeds ≥ 7 m s^{-1}, and no sea ice, there was almost calcium depletion (EF_{Ca}, M ± SD = 1.01 ± 0.80, median = 0.70, IQR = 0.73, n = 182) in the SSA (Fig. S6).

We noted that a series of high EF_{Ca} cases (Area 1) were correlated with a high concentration of chlorophyll-a (0.99 ± 1.65 μg L^{-1}) during leg II (Fig. S7 and Table S4). However, the enhanced EF_{Ca} was unlikely to be attributed to phytoplankton and/or bacteria due to the poor correlation ($r = 0.12$, $p < 0.01$) between the chlorophyll-a concentration and EF_{Ca} values (Fig. S8). Moreover, the ship track of leg II covered large areas with higher chlorophyll-a concentrations, but the high EF_{Ca} values only present at the narrow temporal and spatial scales. Therefore, the chlorophyll-a concentration may have a limited impact on Ca^{2+} enrichment.

3.2 Single-particle characteristics of Ca-containing particles

To elucidate the mixing state of individual calcareous particles, all the single-particle types that were obtained from ART-2a were further refined with an ion signal of *m/z* 40 $[Ca]^+$. A total of ~ 580, 000 Ca-containing particles were distributed among all particle types, accounting for ~ 62% of the total obtained particles. In particular, OC-Ca was the dominant (~ 72%) particle type among

https://doi.org/10.5194/egusphere-2023-322
Preprint. Discussion started: 24 March 2023

all Ca-containing particles, followed by SS-Ca (calcium-containing sea salt, ~ 12%) (Fig. 3). Each of the remaining particle types accounted for negligible fractions (< 7%) in the total of Ca-containing particles, and were classified as "Other", thus, they are not included in the following discussion.

OC-Ca is characterized by a prominent ion signature for *m/z* at 40 $[Ca]^+$ in the positive mass spectrum and organic marker ions of biological origin (e.g., organic nitrogen, phosphate, carbohydrate, siliceous materials and organic carbon) in the negative spectrum (Fig. 3). Specifically, organic nitrogen (*m/z* -26 $[CN]^-$ and -42 $[CNO]^-$) shows the largest number fraction (NF) at ~88% (Fig. S5), which is likely derived from organic nitrogen species, such as amines amino groups, and/or cellulose (Czerwieniec et al., 2005; Srivastava et al., 2005; Köllner et al., 2017; Dall'osto et al., 2019). Higher NFs of phosphate (16%; *m/z* -63 $[PO_2]^-$ and -79 $[PO_3]^-$), carbohydrates (24%; *m/z* -45 $[CHO_2]^-$, -59 $[C_2H_3O_2]^-$, and -73 $[C_3H_5O_2]^-$), siliceous materials (40%; *m/z* -60 $[SiO_2]^-$), and organic carbon (37%; *m/z* 27 $[C_2H_3]^-$ and 43 $[C_2H_3O_3]^-$) were also observed in OC-Ca relative to other particle types (Fig. S5). These organic ion signatures likely correspond to phospholipids, mono- and polysaccharides, and biosilica structures (e.g., exoskeletons or frustules), which may be derived from the intact heterotrophic cells, fragments of cells, and exudates of phytoplankton and/or bacterial (Prather et al., 2013; Guasco et al., 2014; Zhang et al., 2018). Besides, the strong organic ion intensities may truly reflect the amount of organic material in OC-Ca, because the particles were sufficiently dry during the ionization process (i.e., complete positive and negative mass spectra) (Gross et al., 2000). Notably, the possible ion signals of bromide (*m/z* -79 and -81) were observed in OC-Ca, indicating a potential source of blowing snow (Yang et al., 2008; Song et al., 2022).

https://doi.org/10.5194/egusphere-2023-322
Preprint. Discussion started: 24 March 2023

The OC-Ca particles were most likely classified as a distinct SSA population, probably of marine biogenic origin. Sea salt particles typically exhibit a stronger *m/z* 23 $[Na]^+$ than *m/z* 40 $[Ca]^+$ due to the higher concentration of Na^+ vs. Ca^{2+} in seawater and also due to the lower ionization potential of Na vs. Ca (5.14 eV vs. 6.11 eV) (Gross et al., 2000). However, the ratio of *m/z* 23 $[Na]^+$ to *m/z* 40 $[Ca]^+$ present in the OC-Ca particles is reversed, verifying a distinct single particle type (Gross et al., 2000; Gaston et al., 2011). Similarly, the ion signal of *m/z* 39 $[K]^+$ does not surpass that of *m/z* 40 $[Ca]^+$ in OC-Ca, although K ionized more easily that Ca (4.34 eV vs. 6.11eV) (Gross et al., 2000). The presence of calcium together with organic species (e.g., organic nitrogen, phosphate, etc.) in SSA verifies a marine-biogenic origin of OC-Ca (Köllner et al., 2021). Although RH at the sampling outlet was < 40%, the short residence time of the particles within the drying tube (< 5 s) and vacuum system (< 1 ms) could have been insufficient for the complete efflorescence of SSA (Gaston et al., 2011; Sierau et al., 2014). Hence, the OC-Ca could not be attributed to the chemical fractionation of the efflorescence SSA in SPAMS analysis. Additionally, based on the single-particle mass spectrometry technique, some particle types with similar chemical characteristics to OC-Ca have been observed in both field and laboratory studies (e.g., atomization of sea ice meltwater collected in the Southern Ocean) (Gaston et al., 2011; Prather et al., 2013; Collins et al., 2014; Guasco et al., 2014; Dall'osto et al., 2019; Su et al., 2021). The OC-Ca may be from local emissions because the measurements were almost entirely influenced by polar air masses (Fig. S1). Other possible sources, such as glacial dust (Tobo et al., 2019), could be excluded because of the lack of crustal mass spectral characteristics (e.g., -76 $[SiO_3]^-$, 27 $[Al]^+$, and 48 $[Ti]^+$/64 $[TiO]^+$) (Pratt et al., 2009; Zawadowicz et al., 2017). The mean mass concentration ratio of Ca/Na in aerosol sample was only 0.10, much lower than that in crust (1.78, w/w).

https://doi.org/10.5194/egusphere-2023-322
Preprint. Discussion started: 24 March 2023

In contrast, SS-Ca was classified as a pure inorganic cluster with predominant contributions of Na-related compounds (*m/z* 23 $[Na]^+$, 46 $[Na_2]^+$, 81/83 $[Na_2{}^{35/37}Cl]^+$, and -93/-95 $[Na^{35/37}Cl_2]^-$), Mg (*m/z* 24), K (*m/z* 39), and Ca (*m/z* 40) in the mass spectra (Fig. 3). Organic ion signals such as organic nitrogen (*m/z* -26 $[CN]^-$ and -42 $[CNO]^-$) and phosphate (*m/z* -63 $[PO_2]^-$ and -79 $[PO_3]^-$) were rarely detected (~1%, by NF). These compounds related to oceanic biogeochemical processes. In addition, secondary species (e.g., nitrate of *m/z* -62 $[NO_3]^-$ and sulfate of *m/z* -97 $[HSO_4]^-$) were also not observed, indicating a fresh origin and/or less atmospheric aging. As a subpopulation of SS, SS-Ca may originate from bubble bursting within open-water and/or blowing snow.

4 Discussion

SS-Ca (calcium-containing sea salt) represents a mixture of NaCl and $CaCl_2$. However, the SS-Ca showed a weak correlation ($r = 0.21$, $p < 0.05$, by count and $r = 0.03$, $p < 0.05$, by peak area of *m/z* 40 $[Ca]^+$) with the mass concentration of Ca^{2+} (Table S5). In addition, the proportion of SS-Ca is also small (11.6%). These results indicated that $CaCl_2$ is not the major cause of the Ca^{2+} enrichment in SSA, although $CaCl_2$ has been proposed as a cause, based on laboratory atomizing of pure inorganic artificial seawater (Salter et al., 2016). The contribution of ikaite ($CaCO_3 \cdot 6H_2O$) could also be excluded due to its low water solubility (Bischoff et al., 1993; Dieckmann et al., 2008; Dieckmann et al., 2010), although ikaite from sea salt fractionation has also been proposed to account for the Ca^{2+} enrichment in the SSA over the Antarctic coast (Hara et al., 2012). Moreover, the mass spectral signatures of $CaCO_3$ (e.g., *m/z* 56 $[CaO]^+$ and -60 $[CO_3]^{2-}$ (see Sullivan et al. (2009)) were also rare in the SS-Ca particles (Fig. 3).

https://doi.org/10.5194/egusphere-2023-322
Preprint. Discussion started: 24 March 2023

As a major component (~ 72%) of the Ca-containing particles, OC-Ca was expected to be partly responsible for the calcium enrichment in SSA. First, the OC-Ca and mass concentration of Ca^{2+} exhibited moderately weak positive correlations (r = 0.42, $p < 0.05$, by count and r = 0.49, $p < 0.05$, by peak area of *m/z* 40 $[Ca]^+$) (Table S5) and moderately strong correlations under higher EF_{Ca} values ($EF_{Ca} > 10$, r = 0.63, $p < 0.05$, by count and r = 0.68, $p < 0.05$, by peak area of *m/z* 40 $[Ca]^+$) (Table S5 and SI text S6). Second, the OC-Ca showed a size distribution with a peak at 1 μm (Fig. 3), which is consistent with the significant Ca^{2+} enrichment that is generally found in submicron SSA (Cochran et al., 2016; Salter et al., 2016; Mukherjee et al., 2020).

We further show that calcium may strongly mix with organic matter, probably as organically complexed calcium, in the OC-Ca particles. The calcium was well correlated with different kinds of organic matter (e.g., phosphate, r = 0.81, $p < 0.05$, by peak area), but poorly correlated with chloride (r = 0.21, $p < 0.05$, by peak area and r = 0.48, $p < 0.05$, by mass concentration) (Fig. S9). In addition, different kinds of organic matter (e.g., organic nitrogen, organic carbon, etc.) in the OC-Ca particles also showed enrichment trends below the submicron level, analogously to Ca^{2+} enrichment (Fig. S10). Particularly, EF_{Ca} and organic nitrogen (with the largest NF in OC-Ca) were both affected by the environmental factors of ambient temperature, wind speed, and sea ice fraction, indicating possible organic binding with calcium (Fig. S11).

To exclude the potential inorganic water-soluble compounds (i.e., chloride (*m/z* -35 and -37), nitrate (*m/z* -62), and sulfate (*m/z* -97)), we further classified OC-Ca into two subpopulations, OC-Ca-Organic (23.6%, by proportion) and OC-Ca-Inorganic (48.7%, by proportion) (Fig. S12), depending on the presence of inorganic ion signals (i.e., chloride of *m/z* -35/-37 $[Cl]^-$, nitrate of *m/z* -62 $[NO_3]^-$, and sulfate of *m/z* -97 $[HSO_4]^-$). Both the OC-Ca types and mass concentrations of

https://doi.org/10.5194/egusphere-2023-322
Preprint. Discussion started: 24 March 2023

Ca^{2+} showed enhanced correlations under high EF_{Ca} values (Table S5). In particular, OC-Ca-Organic exhibited stronger correlations than did OC-Ca-Inorganic (r = 0.51 vs. r = 0.28, $p < 0.05$, by count and r = 0.51 vs. 0.31, $p < 0.05$, by peak area of *m/z* 40 $[Ca]^+$, respectively), which indicated the importance of OC-Ca-Organic for the enrichment of Ca^{2+}. That is, the organically complexed calcium may have a certain water solubility and partly responsible for calcium enrichment, while current studies may neglect it.

The possible processes contributing to the calcium enrichment induced by OC-Ca are illustrated in Fig. 4. Ca^{2+} tends to bind with organic matter of biogenic origin, such as exopolymer substances (EPSs), and subsequently assemble as marine microgels (Verdugo et al., 2004; Gaston et al., 2011; Krembs et al., 2011; Orellana et al., 2011; Verdugo, 2012; Orellana et al., 2021). Due to its porous nature, the sea ice sticks to the abundant microgels that are driven by sea ice algae, microorganisms, and/or exchanges of organic matter with the seawater below, which are likely present in the snow, frost flowers, and brine channels (Krembs et al., 2002; Gao et al., 2012; Vancoppenolle et al., 2013; Arrigo, 2014; Boetius et al., 2015; Kirpes et al., 2019). A low wind speed may not only be conducive to the formation of frost flowers and snow but also produce less sea salt (i.e., small yields of Na^+ relative to Ca^{2+}) (Rankin et al., 2002). Correspondingly, a high wind speed (≥ 7 m s^{-1}) yields more sea salt by blowing-snow events and/or wave breaking (Yang et al., 2008; Song et al., 2022), presenting a dilution effect of Na^+ on Ca^{2+}. In this case, the calcium enrichment in SSA could reasonably be attributed to the gel-like calcium particles (higher proportion of OC-Ca at low wind speeds (< 7 m s^{-1}, 61.5%) relative to high wind speeds (≥ 7 m s^{-1}, 38.5%)). Coincidently, Song et al. (2022) also reported that low wind-blown sea ice process can drive the biogenic aerosol response in the high Arctic area. In addition, the enhanced presence of

https://doi.org/10.5194/egusphere-2023-322
Preprint. Discussion started: 24 March 2023

film drops was observed at lower wind speeds (< 6 m s^{-1}) (Norris et al., 2011), which suggest that the bubble bursts within the sea ice leads and open-water may also be responsible for the release of OC-Ca and its calcium enrichment involved (Leck and Bigg, 2005b, a; Bigg and Leck, 2008; Leck and Bigg, 2010; Leck et al., 2013; Kirpes et al., 2019).

Noticeable, it is still quite a challenge to obtain quantitative measurements using SPAMS due to the potential inhomogeneities in the transmission efficiencies of the aerodynamic lenses and desorption/ionization, and the matrix effects of individual particles (Gross et al., 2000; Qin et al., 2006; Pratt and Prather, 2012). SPAMS cannot measure the Aitken-mode particles (Sierau et al., 2014), it can measure only the tail of accumulation-mode particles with relatively low hit rate (~11% in this study). Additionally, there is a difference in the size of collected particles between SPAMS (0.2–2 μm) and IGAC (~ 10 μm). Meanwhile, IGAC may partly reflect the Ca^{2+} distribution based the water-soluble Ca^{2+} as OC-Ca may have a low water solubility. Therefore, it may not be straightforward to use the particle count and peak area in comparison with the absolute mass concentration. Nevertheless, our results successfully identified a unique calcareous particle type (i.e., OC-Ca) and its specific mixing state, which provides some insights into the mechanisms behind calcium enrichment.

5 Conclusions

We investigated the distribution of calcium in SSA through the R/V *Xuelong* cruise observations over the Ross Sea, Antarctica. The most significant Ca^{2+} enrichment in SSA occurred under relatively lower ambient temperatures (< -3.5 ℃) and wind speeds (< 7 m s^{-1}) and with the presence of sea ice. With the help of individual particle mass spectral analysis, we first proposed

https://doi.org/10.5194/egusphere-2023-322
Preprint. Discussion started: 24 March 2023

that a single-particle type of OC-Ca (internally mixed organics with calcium), probably resulting from the preferential binding of Ca^{2+} with organic matter, could partly account for the calcium enrichment in SSA. We inferred that OC-Ca is likely produced from the effects of low wind-blown sea ice on microgels induced by Ca^{2+} and/or the bubble bursts in the open-water and/or sea ice leads. However, the impact of environmental factors and OC-Ca on calcium enrichment in SSA still cannot be well predicted by multiple linear regression and random forest analysis (SI text S7), which may be ascribed to other unknown mechanisms and/or organically complexed calcium with a low water solubility. In addition, our conclusions based on limited spatial and temporal conditions may not be accessible to other seasons and oceanic basins.

We suggest that the environmental behaviors of the possible gel-like calcium particles (i.e., OC-Ca) should be paid more attention behind the mechanisms of calcium enrichment. To our knowledge, this is the first report of a calcium-dominated single-particle type OC-Ca in the Antarctic. Such particles may be preferred candidates for CCN and/or IN (Willis et al., 2018; Lawler et al., 2021). In the context of global warming and sea ice retreat, this work provides insight into the chemical composition and distribution of submicron SSA in the Antarctic summer atmosphere, which would be helpful for a better understanding of aerosol-cloud-climate interactions.

Data Availability Statement

The data are available at Zenodo (https://doi.org/10.5281/zenodo.7276073).

Declaration of Competing Interest

The authors declare that they have no known competing financial interests or personal

https://doi.org/10.5194/egusphere-2023-322
Preprint. Discussion started: 24 March 2023

relationships that could have appeared to influence the work reported in this paper.

Author Contributions

The idea for the study was conceived by BJS. BJS analyzed the data, prepared the figures, and wrote the manuscript under the guidance of GHZ and XYB. LL and JPY contributed to the observation data. All co-authors contributed to the discussions of the results and refinement of the manuscript.

Acknowledgment

This work was supported by the Guangdong Basic and Applied Basic Research Foundation (2019B151502022), the National Natural Science Foundation of China (42077322 and 42130611), the Youth Innovation Promotion Association CAS (2021354), and the Guangdong Foundation for Program of Science and Technology Research (2020B1212060053).

https://doi.org/10.5194/egusphere-2023-322
Preprint. Discussion started: 24 March 2023

375 **Figure captions**

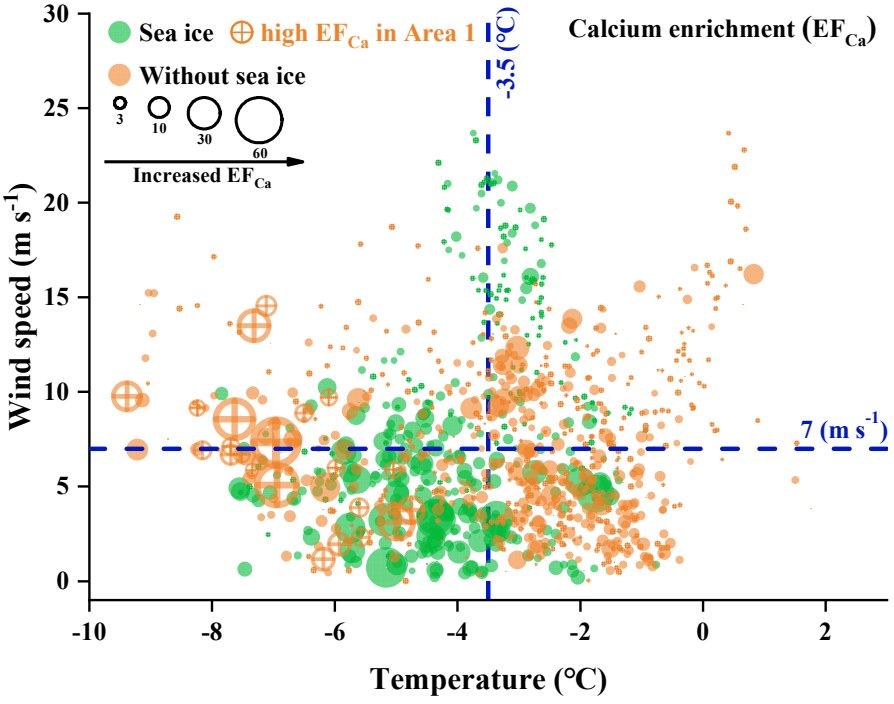

376

377 **Figure 1**

378 Bubble chart of the hourly Ca^{2+} enrichment factor (EF_{Ca}) with respect to Na^{+} with different
379 environmental factors (ambient temperature, wind speed, and sea ice fraction). The green and
380 orange dots represent the EF_{Ca} values for the periods with and without sea ice, respectively. The
381 orange marked dots represent a series of high EF_{Ca} cases that were correlated with a high
382 concentration of chlorophyll-a during leg II of the cruise.

https://doi.org/10.5194/egusphere-2023-322
Preprint. Discussion started: 24 March 2023

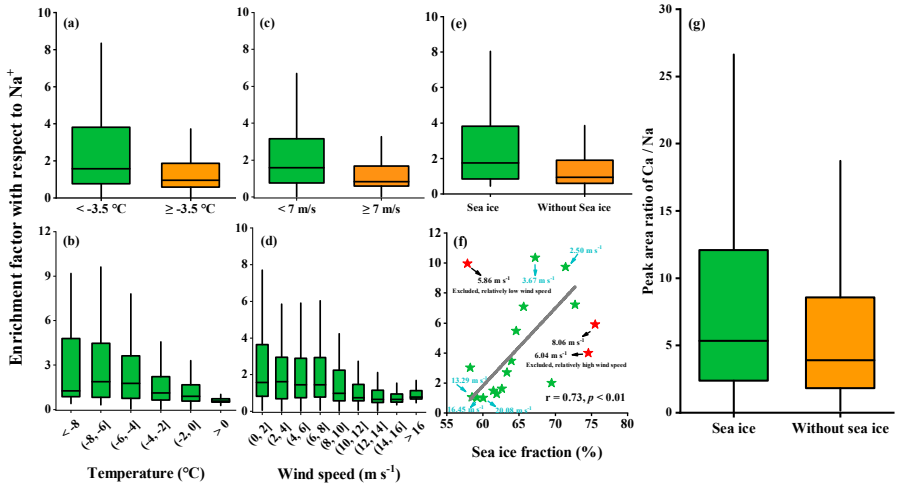

Figure 2

Enrichment factors of Ca^{2+} with respect to Na^{+} varied as a function of the ambient temperature (a-b), wind speed (c-d), and sea ice fraction (e-f) during cruise observations. (g) A box and whisker plot of the single-particle peak area ratio of Ca/Na in OC-Ca for the periods with and without sea ice. In the box and whisker plots, the lower, median, and upper lines of the box denote the 25th, 50th and 75th percentiles, respectively. The lower and upper edges denote the 10th and 90th percentiles, respectively. The black solid star (f) exhibited an anomalous trend due to its nature of the relatively high or low wind speed. The first point exhibited a high EF value because of its relatively low wind speed (5.86 m s^{-1}). The second and third points exhibited low EF values because of their relatively high wind speeds of 6.04 m s^{-1} and 8.06 m s^{-1}, respectively. These three points have been excluded in the correlation analysis.

https://doi.org/10.5194/egusphere-2023-322
Preprint. Discussion started: 24 March 2023

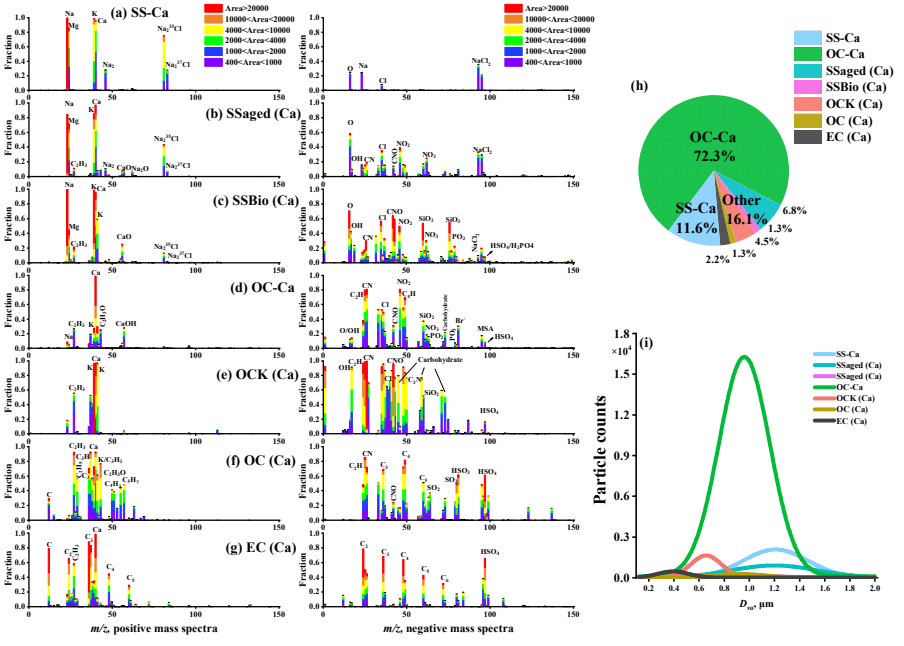

Figure 3

(a) – (g) Average digitized single-particle mass spectra of seven chemical classes of Ca-containing particles. New particle types are reclassified with *m/z* 40 [Ca^{2+}] based on previous ART-2a results. (h) Relative proportion and (i) unscaled size-resolved number distributions of these single-particle types.

https://doi.org/10.5194/egusphere-2023-322
Preprint. Discussion started: 24 March 2023

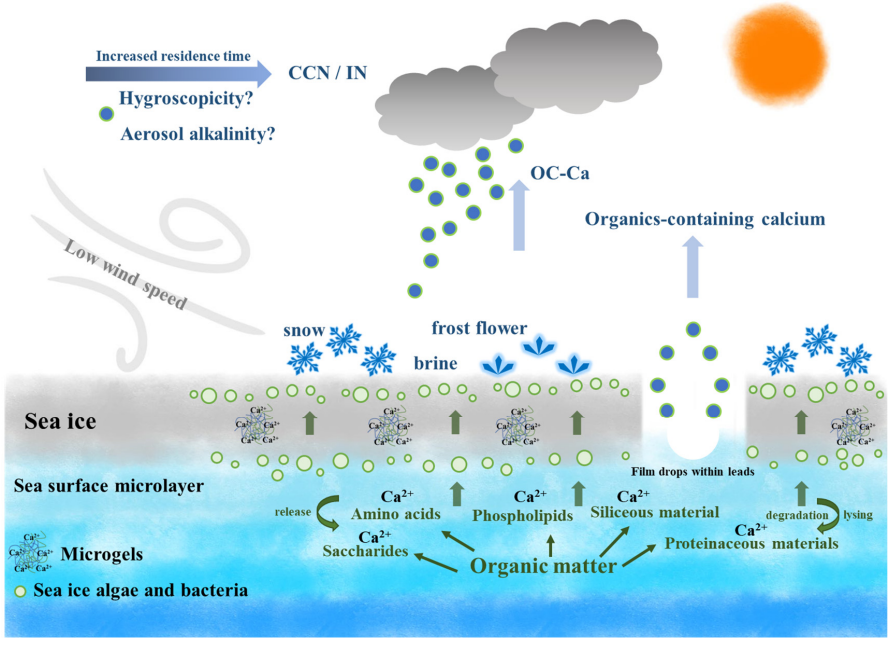

Figure 4

Schematic of the production of OC-Ca and its possible atmospheric implications beyond calcium enrichment. Ca^{2+} tends to bind with organic matter whining sea ice/seawater, and subsequently assemble to marine microgels, likely present in the snow, frost flowers, and brine channels. With the low wind-blown sea ice process and/or bubble bursting within sea ice leads, these gel-like particles (i.e., OC-Ca) may be released to the Antarctic atmosphere, as a potential source of CCN/IN.

https://doi.org/10.5194/egusphere-2023-322
Preprint. Discussion started: 24 March 2023

References

Arrigo, K. R.: Sea ice ecosystems, Ann Rev Mar Sci, 6, 439-467, https://doi.org/10.1146/annurev-marine-010213-135103, 2014.

Bertram, T. H., Cochran, R. E., Grassian, V. H., and Stone, E. A.: Sea spray aerosol chemical composition: elemental and molecular mimics for laboratory studies of heterogeneous and multiphase reactions, Chemical Society Reviews, 47, 2374-2400, https://doi.org/10.1039/c7cs00008a, 2018.

Bigg, E. K. and Leck, C.: The composition of fragments of bubbles bursting at the ocean surface, Journal of Geophysical Research: Atmospheres, 113https://doi.org/10.1029/2007jd009078, 2008.

Bischoff, J. L., Fitzpatrick, J. A., and Rosenbauer, R. J.: The Solubility and Stabilization of Ikaite (Caco3.6h2o) from 0-Degrees-C To 25-Degrees-C - Environmental and Paleoclimatic Implications for Thinolite Tufa, J Geol, 101, 21-33, https://doi.org/10.1086/648194, 1993.

Boetius, A., Anesio, A. M., Deming, J. W., Mikucki, J. A., and Rapp, J. Z.: Microbial ecology of the cryosphere: sea ice and glacial habitats, Nat Rev Microbiol, 13, 677-690, https://doi.org/10.1038/nrmicro3522, 2015.

Boreddy, S. K. R. and Kawamura, K.: A 12-year observation of water-soluble ions in TSP aerosols collected at a remote marine location in the western North Pacific: an outflow region of Asian dust, Atmos Chem Phys, 15, 6437-6453, https://doi.org/10.5194/acp-15-6437-2015, 2015.

Brooks, S. D. and Thornton, D. C. O.: Marine Aerosols and Clouds, Annu Rev Mar Sci, 10, 289-313, https://doi.org/10.1146/annurev-marine-121916-063148, 2018.

Carter-Fenk, K. A., Dommer, A. C., Fiamingo, M. E., Kim, J., Amaro, R. E., and Allen, H. C.: Calcium bridging drives polysaccharide co-adsorption to a proxy sea surface microlayer, Phys Chem Chem Phys, 23, 16401-16416, https://doi.org/10.1039/d1cp01407b, 2021.

Chi, J. W., Li, W. J., Zhang, D. Z., Zhang, J. C., Lin, Y. T., Shen, X. J., Sun, J. Y., Chen, J. M., Zhang, X. Y., Zhang, Y. M., and Wang, W. X.: Sea salt aerosols as a reactive surface for inorganic and organic acidic gases in the Arctic troposphere, Atmos Chem Phys, 15, 11341-11353, https://doi.org/10.5194/acp-15-11341-2015, 2015.

Cochran, R. E., Jayarathne, T., Stone, E. A., and Grassian, V. H.: Selectivity Across the Interface: A Test of Surface Activity in the Composition of Organic-Enriched Aerosols from Bubble Bursting, J Phys Chem Lett, 7, 1692-1696, https://doi.org/10.1021/acs.jpclett.6b00489, 2016.

Collins, D. B., Zhao, D. F., Ruppel, M. J., Laskina, O., Grandquist, J. R., Modini, R. L., Stokes, M. D., Russell, L. M., Bertram, T. H., Grassian, V. H., Deane, G. B., and Prather, K. A.: Direct aerosol chemical composition measurements to evaluate the physicochemical differences between controlled sea spray aerosol generation schemes, Atmos Meas Tech, 7, 3667-3683, https://doi.org/10.5194/amt-7-3667-2014, 2014.

Cravigan, L. T., Mallet, M. D., Vaattovaara, P., Harvey, M. J., Law, C. S., Modini, R. L., Russell, L. M., Stelcer, E., Cohen, D. D., Olsen, G., Safi, K., Burrell, T. J., and Ristovski, Z.: Sea spray aerosol organic enrichment, water uptake and surface tension effects, Atmos Chem Phys, 20, 7955-7977, https://doi.org/10.5194/acp-20-7955-2020, 2020.

Czerwieniec, G. A., Russell, S. C., Tobias, H. J., Pitesky, M. E., Fergenson, D. P., Steele, P., Srivastava, A., Horn, J. M., Frank, M., Gard, E. E., and Lebrilla, C. B.: Stable isotope labeling of entire Bacillus atrophaeus spores and vegetative cells using bioaerosol mass spectrometry, Anal Chem, 77, 1081-1087, https://doi.org/10.1021/ac0488098, 2005.

https://doi.org/10.5194/egusphere-2023-322
Preprint. Discussion started: 24 March 2023

Dall'Osto, M., Airs, R. L., Beale, R., Cree, C., Fitzsimons, M. F., Beddows, D., Harrison, R. M., Ceburnis, D., O'Dowd, C., Rinaldi, M., Paglione, M., Nenes, A., Decesari, S., and Simo, R.: Simultaneous Detection of Alkylamines in the Surface Ocean and Atmosphere of the Antarctic Sympagic Environment, Acs Earth Space Chem, 3, 854-862, https://doi.org/10.1021/acsearthspacechem.9b00028, 2019.

Dieckmann, G., Nehrke, G., Uhlig, C., Göttlicher, J., Gerland, S., Granskog, M., and Thomas, D.: Brief Communication: Ikaite (CaCO3·6H2O) discovered in Arctic sea ice, The Cryosphere, 4, 227-230, https://doi.org/10.5194/tc-4-227-2010, 2010.

Dieckmann, G., Nehrke, G., Papadimitriou, S., Göttlicher, J., Steininger, R., Kennedy, H., Wolf-Gladrow, D., and Thomas, D.: Calcium carbonate as ikaite crystals in Antarctic sea ice, Geophys Res Lett, 35https://doi.org/10.1029/2008gl033540, 2008.

Gao, Q., Leck, C., Rauschenberg, C., and Matrai, P. A.: On the chemical dynamics of extracellular polysaccharides in the high Arctic surface microlayer, Ocean Sci, 8, 401-418, https://doi.org/10.5194/os-8-401-2012, 2012.

Gaston, C. J., Furutani, H., Guazzotti, S. A., Coffee, K. R., Bates, T. S., Quinn, P. K., Aluwihare, L. I., Mitchell, B. G., and Prather, K. A.: Unique ocean-derived particles serve as a proxy for changes in ocean chemistry, Journal of Geophysical Research: Atmospheres, 116https://doi.org/10.1029/2010jd015289, 2011.

Gross, D. S., Galli, M. E., Silva, P. J., and Prather, K. A.: Relative sensitivity factors for alkali metal and ammonium cations in single particle aerosol time-of-flight mass spectra, Anal Chem, 72, 416-422, https://doi.org/10.1021/ac990434g, 2000.

Guasco, T. L., Cuadra-Rodriguez, L. A., Pedler, B. E., Ault, A. P., Collins, D. B., Zhao, D. F., Kim, M. J., Ruppel, M. J., Wilson, S. C., Pomeroy, R. S., Grassian, V. H., Azam, F., Bertram, T. H., and Prather, K. A.: Transition Metal Associations with Primary Biological Particles in Sea Spray Aerosol Generated in a Wave Channel, Environ Sci Technol, 48, 1324-1333, https://doi.org/10.1021/es403203d, 2014.

Hara, K., Osada, K., Yabuki, M., and Yamanouchi, T.: Seasonal variation of fractionated sea-salt particles on the Antarctic coast, Geophys Res Lett, 39https://doi.org/10.1029/2012gl052761, 2012.

Keene, W. C., Maring, H., Maben, J. R., Kieber, D. J., Pszenny, A. A. P., Dahl, E. E., Izaguirre, M. A., Davis, A. J., Long, M. S., Zhou, X. L., Smoydzin, L., and Sander, R.: Chemical and physical characteristics of nascent aerosols produced by bursting bubbles at a model air-sea interface, Journal of Geophysical Research: Atmospheres, 112https://doi.org/10.1029/2007jd008464, 2007.

Kirpes, R. M., Bonanno, D., May, N. W., Fraund, M., Barget, A. J., Moffet, R. C., Ault, A. P., and Pratt, K. A.: Wintertime Arctic Sea Spray Aerosol Composition Controlled by Sea Ice Lead Microbiology, Acs Central Sci, 5, 1760-1767, https://doi.org/10.1021/acscentsci.9b00541, 2019.

Köllner, F., Schneider, J., Willis, M. D., Klimach, T., Helleis, F., Bozem, H., Kunkel, D., Hoor, P., Burkart, J., Leaitch, W. R., Aliabadi, A. A., Abbatt, J. P. D., Herber, A. B., and Borrmann, S.: Particulate trimethylamine in the summertime Canadian high Arctic lower troposphere, Atmos Chem Phys, 17, 13747-13766, https://doi.org/10.5194/acp-17-13747-2017, 2017.

Köllner, F., Schneider, J., Willis, M. D., Schulz, H., Kunkel, D., Bozem, H., Hoor, P., Klimach, T., Helleis, F., Burkart, J., Leaitch, W. R., Aliabadi, A. A., Abbatt, J. P. D., Herber, A. B., and Borrmann, S.: Chemical composition and source attribution of sub-micrometre aerosol particles in the summertime Arctic lower troposphere, Atmos Chem Phys, 21, 6509-6539, https://doi.org/10.5194/acp-21-6509-2021, 2021.

https://doi.org/10.5194/egusphere-2023-322
Preprint. Discussion started: 24 March 2023

Krembs, C., Eicken, H., and Deming, J. W.: Exopolymer alteration of physical properties of sea ice and implications for ice habitability and biogeochemistry in a warmer Arctic, P Natl Acad Sci USA, 108, 3653-3658, https://doi.org/10.1073/pnas.1100701108, 2011.

Krembs, C., Eicken, H., Junge, K., and Deming, J. W.: High concentrations of exopolymeric substances in Arctic winter sea ice: implications for the polar ocean carbon cycle and cryoprotection of diatoms, Deep-Sea Res Pt I, 49, 2163-2181, https://doi.org/10.1016/S0967-0637(02)00122-X, 2002.

Lawler, M. J., Saltzman, E. S., Karlsson, L., Zieger, P., Salter, M., Baccarini, A., Schmale, J., and Leck, C.: New Insights Into the Composition and Origins of Ultrafine Aerosol in the Summertime High Arctic, Geophys Res Lett, 48https://doi.org/10.1029/2021gl094395, 2021.

Leck, C. and Bigg, E. K.: Source and evolution of the marine aerosol - A new perspective, Geophys Res Lett, 32https://doi.org/10.1029/2005gl023651, 2005a.

Leck, C. and Bigg, E. K.: Biogenic particles in the surface microlayer and overlaying atmosphere in the central Arctic Ocean during summer, Tellus B, 57, 305-316, https://doi.org/10.1111/j.1600-0889.2005.00148.x, 2005b.

Leck, C. and Bigg, E. K.: New Particle Formation of Marine Biological Origin, Aerosol Sci Tech, 44, 570-577, https://doi.org/10.1080/02786826.2010.481222, 2010.

Leck, C. and Svensson, E.: Importance of aerosol composition and mixing state for cloud droplet activation over the Arctic pack ice in summer, Atmos Chem Phys, 15, 2545-2568, https://doi.org/10.5194/acp-15-2545-2015, 2015.

Leck, C., Gao, Q., Mashayekhy Rad, F., and Nilsson, U.: Size-resolved atmospheric particulate polysaccharides in the high summer Arctic, Atmos Chem Phys, 13, 12573-12588, https://doi.org/10.5194/acp-13-12573-2013, 2013.

Li, L., Huang, Z., Dong, J., Li, M., Gao, W., Nian, H., Fu, Z., Zhang, G., Bi, X., Cheng, P., and Zhou, Z.: Real time bipolar time-of-flight mass spectrometer for analyzing single aerosol particles, Int J Mass Spectrom, 303, 118-124, https://doi.org/10.1016/j.ijms.2011.01.017, 2011.

Mukherjee, P., Reinfelder, J. R., and Gao, Y.: Enrichment of calcium in sea spray aerosol in the Arctic summer atmosphere, Mar Chem, 227https://doi.org/10.1016/j.marchem.2020.103898, 2020.

Murphy, D. M., Anderson, J. R., Quinn, P. K., McInnes, L. M., Brechtel, F. J., Kreidenweis, S. M., Middlebrook, A. M., Posfai, M., Thomson, D. S., and Buseck, P. R.: Influence of sea-salt on aerosol radiative properties in the Southern Ocean marine boundary layer, Nature, 392, 62-65, https://doi.org/10.1038/32138, 1998.

Norris, S. J., Brooks, I. M., de Leeuw, G., Sirevaag, A., Leck, C., Brooks, B. J., Birch, C. E., and Tjernstrom, M.: Measurements of bubble size spectra within leads in the Arctic summer pack ice, Ocean Sci, 7, 129-139, https://doi.org/10.5194/os-7-129-2011, 2011.

Oppo, C., Bellandi, S., Innocenti, N. D., Stortini, A. M., Loglio, G., Schiavuta, E., and Cini, R.: Surfactant components of marine organic matter as agents for biogeochemical fractionation and pollutant transport via marine aerosols, Mar Chem, 63, 235-253, https://doi.org/10.1016/S0304-4203(98)00065-6, 1999.

Orellana, M. V. and Verdugo, P.: Ultraviolet radiation blocks the organic carbon exchange between the dissolved phase and the gel phase in the ocean, Limnol Oceanogr, 48, 1618-1623, https://doi.org/10.4319/lo.2003.48.4.1618, 2003.

Orellana, M. V., Hansell, D. A., Matrai, P. A., and Leck, C.: Marine Polymer-Gels' Relevance in the Atmosphere as Aerosols and CCN, Gels, 7https://doi.org/10.3390/gels7040185, 2021.

https://doi.org/10.5194/egusphere-2023-322
Preprint. Discussion started: 24 March 2023

Orellana, M. V., Matrai, P. A., Leck, C., Rauschenberg, C. D., Lee, A. M., and Coz, E.: Marine microgels as a source of cloud condensation nuclei in the high Arctic, P Natl Acad Sci USA, 108, 13612-13617, https://doi.org/10.1073/pnas.1102457108, 2011.

Prather, K. A., Bertram, T. H., Grassian, V. H., Deane, G. B., Stokes, M. D., DeMott, P. J., Aluwihare, L. I., Palenik, B. P., Azam, F., Seinfeld, J. H., Moffet, R. C., Molina, M. J., Cappa, C. D., Geiger, F. M., Roberts, G. C., Russell, L. M., Ault, A. P., Baltrusaitis, J., Collins, D. B., Corrigan, C. E., Cuadra-Rodriguez, L. A., Ebben, C. J., Forestieri, S. D., Guasco, T. L., Hersey, S. P., Kim, M. J., Lambert, W. F., Modini, R. L., Mui, W., Pedler, B. E., Ruppel, M. J., Ryder, O. S., Schoepp, N. G., Sullivan, R. C., and Zhao, D. F.: Bringing the ocean into the laboratory to probe the chemical complexity of sea spray aerosol, P Natl Acad Sci USA, 110, 7550-7555, https://doi.org/10.1073/pnas.1300262110, 2013.

Pratt, K. A. and Prather, K. A.: Mass spectrometry of atmospheric aerosolsuRecent developments and applications. Part II: On-line mass spectrometry techniques, Mass Spectrom Rev, 31, 17-48, https://doi.org/10.1002/mas.20330, 2012.

Pratt, K. A., DeMott, P. J., French, J. R., Wang, Z., Westphal, D. L., Heymsfield, A. J., Twohy, C. H., Prenni, A. J., and Prather, K. A.: In situ detection of biological particles in cloud ice-crystals, Nat Geosci, 2, 397-400, https://doi.org/10.1038/Ngeo521, 2009.

Qin, X. Y., Bhave, P. V., and Prather, K. A.: Comparison of two methods for obtaining quantitative mass concentrations from aerosol time-of-flight mass spectrometry measurements, Anal Chem, 78, 6169-6178, https://doi.org/10.1021/ac060395q, 2006.

Quinn, P. K., Collins, D. B., Grassian, V. H., Prather, K. A., and Bates, T. S.: Chemistry and Related Properties of Freshly Emitted Sea Spray Aerosol, Chem Rev, 115, 4383-4399, https://doi.org/10.1021/cr500713g, 2015.

Rankin, A. M., Wolff, E. W., and Martin, S.: Frost flowers: Implications for tropospheric chemistry and ice core interpretation, Journal of Geophysical Research: Atmospheres, 107, AAC 4-1-AAC 4-15, https://doi.org/10.1029/2002jd002492, 2002.

Russell, L. M., Hawkins, L. N., Frossard, A. A., Quinn, P. K., and Bates, T. S.: Carbohydrate-like composition of submicron atmospheric particles and their production from ocean bubble bursting, P Natl Acad Sci USA, 107, 6652-6657, https://doi.org/10.1073/pnas.0908905107, 2010.

Salter, M. E., Hamacher-Barth, E., Leck, C., Werner, J., Johnson, C. M., Riipinen, I., Nilsson, E. D., and Zieger, P.: Calcium enrichment in sea spray aerosol particles, Geophys Res Lett, 43, 8277-8285, https://doi.org/10.1002/2016gl070275, 2016.

Sierau, B., Chang, R. Y. W., Leck, C., Paatero, J., and Lohmann, U.: Single-particle characterization of the high-Arctic summertime aerosol, Atmos Chem Phys, 14, 7409-7430, https://doi.org/10.5194/acp-14-7409-2014, 2014.

Sievering, H.: Aerosol non-sea-salt sulfate in the remote marine boundary layer under clear-sky and normal cloudiness conditions: Ocean-derived biogenic alkalinity enhances sea-salt sulfate production by ozone oxidation, Journal of Geophysical Research: Atmospheres, 109https://doi.org/10.1029/2003jd004315, 2004.

Song, C., Becagli, S., Beddows, D. C. S., Brean, J., Browse, J., Dai, Q., Dall'Osto, M., Ferracci, V., Harrison, R. M., Harris, N., Li, W., Jones, A. E., Kirchgäßner, A., Kramawijaya, A. G., Kurganskiy, A., Lupi, A., Mazzola, M., Severi, M., Traversi, R., and Shi, Z.: Understanding Sources and Drivers of Size-Resolved Aerosol in the High Arctic Islands of Svalbard Using a Receptor Model Coupled with Machine Learning, Environ Sci Technol, 56, 11189-11198,

https://doi.org/10.5194/egusphere-2023-322
Preprint. Discussion started: 24 March 2023

https://doi.org/10.1021/acs.est.1c07796, 2022.

Song, X. and Hopke, P. K.: Classification of single particles analyzed by ATOFMS using an artificial neural network, ART-2A, Anal Chem, 71, 860-865, https://doi.org/10.1021/ac9809682, 1999.

Srivastava, A., Pitesky, M. E., Steele, P. T., Tobias, H. J., Fergenson, D. P., Horn, J. M., Russell, S. C., Czerwieniec, G. A., Lebrilla, C. S., Gard, E. E., and Frank, M.: Comprehensive assignment of mass spectral signatures from individual Bacillus atrophaeus spores in matrix-free laser desorption/ionization bioaerosol mass spectrometry, Anal Chem, 77, 3315-3323, https://doi.org/10.1021/ac048298p, 2005.

Su, B., Wang, T., Zhang, G., Liang, Y., Lv, C., Hu, Y., Li, L., Zhou, Z., Wang, X., and Bi, X.: A review of atmospheric aging of sea spray aerosols: Potential factors affecting chloride depletion, Atmos Environ, 290https://doi.org/10.1016/j.atmosenv.2022.119365, 2022.

Su, B. J., Zhuo, Z. M., Fu, Y. Z., Sun, W., Chen, Y., Du, X. B., Yang, Y. X., Wu, S., Xie, Q. H., Huang, F. G., Chen, D. H., Li, L., Zhang, G. H., Bi, X. H., and Zhou, Z.: Individual particle investigation on the chloride depletion of inland transported sea spray aerosols during East Asian summer monsoon, Sci Total Environ, 765https://doi.org/10.1016/j.scitotenv.2020.144290, 2021.

Sullivan, R. C., Moore, M. J. K., Petters, M. D., Kreidenweis, S. M., Roberts, G. C., and Prather, K. A.: Timescale for hygroscopic conversion of calcite mineral particles through heterogeneous reaction with nitric acid, Phys Chem Chem Phys, 11, 7826-7837, https://doi.org/10.1039/b904217b, 2009.

Tobo, Y., Adachi, K., DeMott, P. J., Hill, T. C. J., Hamilton, D. S., Mahowald, N. M., Nagatsuka, N., Ohata, S., Uetake, J., Kondo, Y., and Koike, M.: Glacially sourced dust as a potentially significant source of ice nucleating particles, Nat Geosci, 12, 253-258, https://doi.org/10.1038/s41561-019-0314-x, 2019.

Vancoppenolle, M., Meiners, K. M., Michel, C., Bopp, L., Brabant, F., Carnat, G., Delille, B., Lannuzel, D., Madec, G., Moreau, S., Tison, J.-L., and van der Merwe, P.: Role of sea ice in global biogeochemical cycles: emerging views and challenges, Quaternary Science Reviews, 79, 207-230, https://doi.org/10.1016/j.quascirev.2013.04.011, 2013.

Verdugo, P.: Marine microgels, Annual Review of Marine Science, 4, 375-400, https://doi.org/10.1146/annurev-marine-120709-142759, 2012.

Verdugo, P., Alldredge, A. L., Azam, F., Kirchman, D. L., Passow, U., and Santschi, P. H.: The oceanic gel phase: a bridge in the DOM-POM continuum, Mar Chem, 92, 67-85, https://doi.org/10.1016/j.marchem.2004.06.017, 2004.

Willis, M. D., Leaitch, W. R., and Abbatt, J. P. D.: Processes Controlling the Composition and Abundance of Arctic Aerosol, Rev Geophys, 56, 621-671, https://doi.org/10.1029/2018rg000602, 2018.

Wilson, T. W., Ladino, L. A., Alpert, P. A., Breckels, M. N., Brooks, I. M., Browse, J., Burrows, S. M., Carslaw, K. S., Huffman, J. A., Judd, C., Kilthau, W. P., Mason, R. H., McFiggans, G., Miller, L. A., Najera, J. J., Polishchuk, E., Rae, S., Schiller, C. L., Si, M., Temprado, J. V., Whale, T. F., Wong, J. P., Wurl, O., Yakobi-Hancock, J. D., Abbatt, J. P., Aller, J. Y., Bertram, A. K., Knopf, D. A., and Murray, B. J.: A marine biogenic source of atmospheric ice-nucleating particles, Nature, 525, 234-238, https://doi.org/10.1038/nature14986, 2015.

Yan, J., Jung, J., Lin, Q., Zhang, M., Xu, S., and Zhao, S.: Effect of sea ice retreat on marine aerosol emissions in the Southern Ocean, Antarctica, Sci Total Environ, 745, 140773, https://doi.org/10.1016/j.scitotenv.2020.140773, 2020a.

Yan, J., Jung, J., Zhang, M., Xu, S., Lin, Q., Zhao, S., and Chen, L.: Significant Underestimation of

https://doi.org/10.5194/egusphere-2023-322
Preprint. Discussion started: 24 March 2023

Gaseous Methanesulfonic Acid (MSA) over Southern Ocean, Environ Sci Technol, 53, 13064-13070, https://doi.org/10.1021/acs.est.9b05362, 2019.

Yan, J., Jung, J., Zhang, M., Bianchi, F., Tham, Y., Xu, S., Lin, Q., Zhao, S., Li, L., and Chen, L.: Uptake selectivity of methanesulfonic acid (MSA) on fine particles over polynya regions of the Ross Sea, Antarctica, Atmos Chem Phys, 20, 3259-3271, https://doi.org/10.5194/acp-20-3259-2020, 2020b.

Yang, X., Pyle, J. A., and Cox, R. A.: Sea salt aerosol production and bromine release: Role of snow on sea ice, Geophys Res Lett, 35https://doi.org/10.1029/2008gl034536, 2008.

Zawadowicz, M. A., Froyd, K. D., Murphy, D. M., and Cziczo, D. J.: Improved identification of primary biological aerosol particles using single-particle mass spectrometry, Atmos Chem Phys, 17, 7193-7212, https://doi.org/10.5194/acp-17-7193-2017, 2017.

Zhang, T., Fiamingo, M., and Allen, H. C.: Trace Metal Enrichment Driven by Phosphate Functional Group Binding Selectivity, Journal of Geophysical Research: Oceans, 123, 5286-5297, https://doi.org/10.1029/2018jc013926, 2018.